Size Dependence of Incipient Dislocation Plasticity in Ni_3Al

L. Zuo, A. H. W. Ngan, and G. P. Zheng

Department of Mechanical Engineering, The University of Hong Kong, Pokfulam Road, Hong Kong, People's Republic of China

(Received 22 December 2004; published 11 March 2005)

Molecular dynamics simulations are carried out to study the incipient dislocation plasticity in Ni_3Al. Dislocation nucleation is found to occur preferentially at energetic atomic clusters with larger-than-average relative displacements. From the simulated distribution of the atomic relative displacements, a scaling model is proposed to predict the size dependence of the incipient plasticity condition in real-sized specimens.

DOI: 10.1103/PhysRevLett.94.095501 PACS numbers: 61.72.Cc, 62.20.Fe

The rapid development of technologies involving micro- and nanomachinery calls for an urgent need to understand material behaviors at the submicron length scale. There is now rather convincing evidence showing that crystalline materials in general exhibit much higher strengths than their bulk counterparts [1,2]. In certain modes of deformation such as torsion, strain gradients are present which lead to a size-dependent hardening effect due to geometrically necessary dislocations [1]. The high strengths of small, annealed specimens, on the other hand, have been observed in early tensile experiments on annealed whisker crystals [3]. This phenomenon is attributed to the scarcity of source dislocations in very small samples, and so dislocations have to be generated from the perfect crystal environment at high stresses. Recently, Uchic *et al.* [2] compressed micropillars of Ni and Ni_3Al fabricated by the focused-ion-beam method and observed a marked increase of yield strength as the specimen size decreases. Incipient plasticity is also easily observable in nanoindentation on annealed, bulk crystalline materials as a load drop or displacement jump [4], and recent experiments show that the statistical distributions of the strain-burst loads in SiC [5] and Ni_3Al [6] obey characteristics of homogeneous nucleation at room temperature. Nanoindentation experiments on annealed Fe-3%Si [4], Ni_3Al [6,7], and Al [8] have also shown that, even if the applied stress is initially in the elastic range, yielding may occur rather suddenly after a certain waiting time, implying that these materials cannot indefinitely sustain GPa-level stresses in the elastic range [9].

In this Letter, we report a theoretical study on the nucleation of defects in a highly stressed crystal at finite temperatures using molecular dynamics simulation. Homogeneous nucleation of dislocations has been studied by Li and co-workers [10,11] as a form of an unstable phonon process under a high applied stress. In the present work, we focus on temperature effects as well as the physical forms of the embryos of the nucleation process.

Simulation model.—The model is set up to mimic the situation of applying homogeneous shear on a small material volume. The aim here is not to simulate directly the behavior of real, micron-sized specimens in real time, as such a task is still too big to be handled by today's computing power. Instead, the purpose of the simulation is to use a sufficiently large block to generate reliable statistical data, for the development of scaling relations to predict real-size and real-time behavior by extrapolation. Before defect generation, the crystal environment is perfect irrespective of block size, and so the material behavior is scalable. We used the embedded atom method potential for Ni_3Al developed by Voter and Chen [12] in the molecular dynamics (MD) simulations. The simulation block consisted of an array of $36 \times 36 \times 24$ atoms, measuring $4.5\ \text{nm} \times 7.4\ \text{nm} \times 10.5\ \text{nm}$, along the three crystallographic directions of $[10\bar{1}]$, [111], and $[1\bar{2}1]$, respectively. Periodic boundary conditions were used along the $[10\bar{1}]$ and $[1\bar{2}1]$ directions, and the (111) surface was left free. The temperature of simulation was controlled at a constant value using a Woodcock thermostat [13]. We applied simple shear by keeping the bottom (111) layer fixed throughout the simulation and fixing a constant velocity to the topmost (111) layer along the $[10\bar{1}]$ direction to achieve a constant strain rate of $5 \times 10^8\ \text{s}^{-1}$. To avoid a shock wave induced by the high strain rate into the block [14], the atoms inside the block were given initial velocities along the $[10\bar{1}]$ direction according to a linear profile along the [111] direction from 0 at the bottom layer to the velocity of the topmost layer.

The system temperature was held at different values ranging from 20 to 600 K during the simulations. We detected the onset of plasticity by looking for sudden relaxation events exhibited by sharp drops in the atomic stress, calculated using Eq. (2.114) in Ref. [15], as well as in the potential energy. To reveal the incipient process, atoms having higher relative displacements with respect to their neighbors [16] are traced. Figures 1(a)–1(c) show a typical incipient process for the simulation at 300 K. Here, only atoms with relative displacements larger than 17% of the lattice constant are plotted. At an applied strain lower than the critical value, certain atomic clusters can be seen to distribute randomly in the block as shown in Fig. 1(a). Most of these energetic atomic clusters, which we refer to as "hot spots" hereafter, will not last for more than

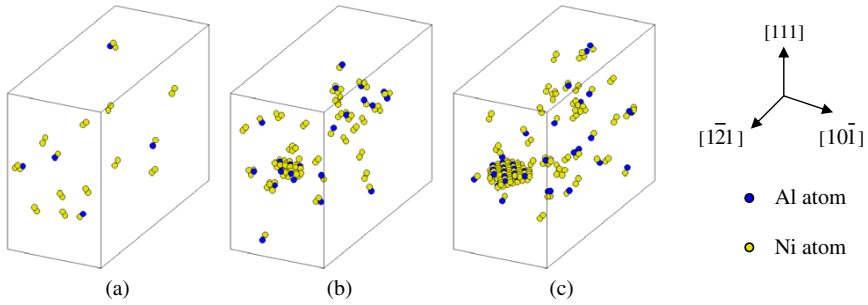

FIG. 1 (color online). Microstructure evolution showing atom clusters with large relative displacements in MD simulation of perfect crystal shearing. (a) Snapshot at simulated strain of $\gamma = 9\%$, showing some hot spots with a relative displacement larger than 17% of a_o beginning to emerge when the stress is about 90% of the critical value. (b) Snapshot at $\gamma = 10.0956\%$, showing a Shockley partial loop ($\mathbf{b} = 1/6[1\bar{2}1]$) being generated from an atom cluster. (A major relaxation event occurred at $\gamma = 10.06\%$.) (c) Snapshot at $\gamma = 10.1052\%$, showing the expansion of this Shockley partial loop during the strain burst.

10 simulation time steps, or 60 fs in real time, of the order of the typical period of atomic vibration, and new hot spots appear after old ones are annihilated. Also, these hot spots are not discrete defects but have rather diffused sizes depending on the critical relative displacement used to define or display them. At or near the critical shear strain of about 10.1%, one or two hot spots may evolve during their limited life span to form a small dislocation loop as shown in Figs. 1(b) and 1(c), and this quickly expanded to cover the whole slip plane in the simulation block. The dislocation was identified to be a Shockley partial dislocation loop with Burgers vector $1/6[1\bar{2}1]$. The eventual expansion of the dislocation loop to form an extended, high-energy complex stacking fault in the ordered $L1_2$ lattice of Ni_3Al may not be very realistic since this is likely to be due to the attractive forces imposed by the periodic boundary conditions. However, the early stage of the nucleation, namely, the evolution of a small loop from a hot spot, should be realistic enough, since cell boundary effects should be small on the hot spot and the small nucleated loop.

In reality, once a small dislocation loop is nucleated, it may cross slip and turn itself into a dislocation source for a subsequent, observable strain burst. The observation in Fig. 1 indicates that a dislocation loop does not nucleate directly from the perfect crystal environment, but a momentarily hot spot has to be involved as a precursor for the nucleation. This explains the experimental observations that, at high indentation loads, the statistical variation of the incipient plasticity process in SiC and Ni_3Al appears to obey homogeneous nucleation kinetics, but nevertheless, the measured activation volumes are atomic rather than the volume expected from a small dislocation loop [5,6]. The activation volumes observed from these experiments are likely to correspond to the hot spots, and, since the occurrence of the hot spots is random, the overall statistical variation of the incipient plasticity process should appear to correspond to homogeneous nucleation as observed.

Scaling model.—To gain a deeper understanding of the nucleation mechanisms involved, we analyze the statistics of the relative displacements of the atoms as follows. It was found that in all the shearing simulations at constant temperatures and at any simulation step before the onset of defect generation, the fraction of atoms having relative displacements higher than a given value x is well describable by the Weibull form:

$$P(x) = \exp[-(x/x_o)^m], \tag{1}$$

where x_o is a normalization constant, but its value is found to change significantly at different time steps and simulated temperatures, and the modulus m is found to remain within a narrow range of about 3.7 ± 0.3 in all the simulations from 20 to 600 K. Figure 2(a) shows an example of the excellent fit of Eq. (1) to a typical set of simulated results at different simulation steps and temperatures. From Eq. (1), the mean relative displacement of the atoms, $\langle x \rangle$, is directly proportional to x_o if m is approximately constant. For example, if $m = 3.7$, $\langle x \rangle = 0.9025 x_o$.

In our simulations, before the generation of defects, the shearing rate used was sufficiently slow so that the shearing process can be regarded as quasistatic. Under this assumption, the simulation step is directly proportional to strain. Figure 2(b) shows the variation of $\langle x \rangle$ at different simulation steps and temperature. These results suggest the following phenomenological relation for x_o:

$$x_o = A(T)\gamma + B(T), \tag{2}$$

where γ is the simulated shear strain on the $\{111\}\langle 01\bar{1}\rangle$ system, and $A(T)$ and $B(T)$ are functions of temperature T only. Physically, Eq. (2) suggests that the mean relative displacement between atoms has two components: the $A\gamma$ component due to the applied strain producing biased relative displacements along the straining direction, and the B component due to thermal agitation producing more isotropic, random relative displacements.

With Eqs. (1) and (2), the criterion for defect generation can be estimated. We first note that the probability function $P(x)$ in Eq. (1) is meant to describe the statistics observed during random sampling over time scales of the order of picoseconds, the typical time scale used in the present MD simulations. In real-time experiments, nucleation of de-

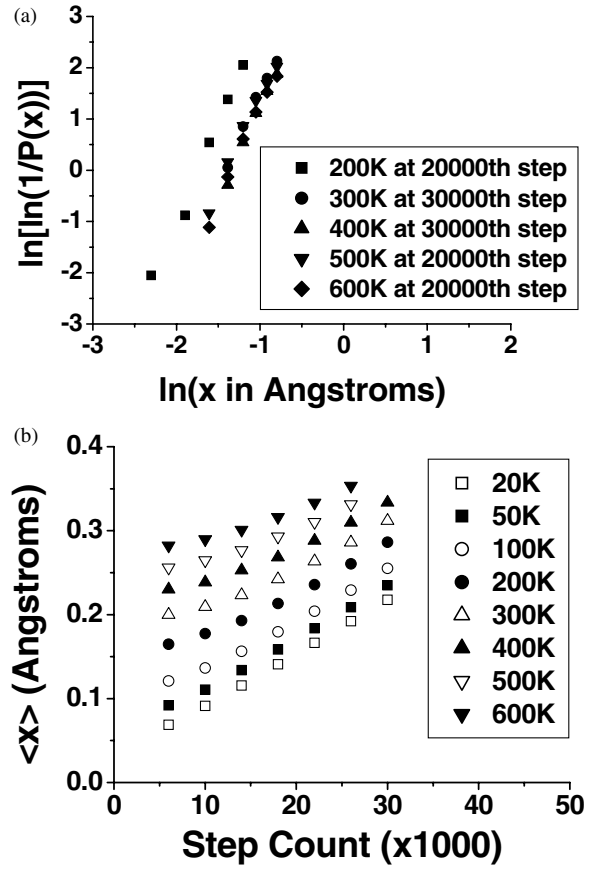

FIG. 2. (a) Weibull plots of typical distributions of atomic relative displacements at different snapshots during constant straining simulations. $P(x)$ is the fraction of atoms displaying relative displacements higher than x. (b) Evolution of mean relative displacements $\langle x \rangle$ at different temperatures.

fects is assisted by thermal agitation and occurs over an average time scale of $\tau \sim (1/\nu)\exp(Q/kT)$, where η is a characteristic atomic vibration frequency, Q is the associated activation energy, and k is the Boltzmann constant. If τ is significantly longer than the MD time scale, so that defect nucleation becomes an extremely rare event, then the probability function $P(x)$ in Eq. (1) would approximate the temporal averaged distribution, although it would give no information on the fluctuations about this average behavior over time scales of the order of τ. From Eq. (1), the temporal average or background maximum relative displacement x_M in the entire material volume is given by

$$1/N = \exp[-(x_M/x_o(\gamma, T))^m], \tag{3}$$

where N is the number of atoms in the material volume, and $x_o(\gamma, T)$ is that given by Eq. (2). We next assume that a defect will be nucleated when the relative displacement of one atom within the material volume reaches approximately one-half of the Shockley partial vector, i.e., when $x = \alpha a_o/\sqrt{6}$, where $\alpha \approx 0.5$ and $a_o = 0.3573$ nm is the lattice constant of Ni_3Al predicted by Voter-Chen potentials [12]. At subcritical conditions, $x_M < \alpha a_o/\sqrt{6}$, and the additional displacement required to reach the unstable point, $(\alpha a_o/\sqrt{6} - x_M)$, has to be provided by thermal agitation. Hence, we assume that the activation energy for defect generation Q can be expressed as a nondecreasing function f of this additional displacement defined over the range $[0, \alpha/\sqrt{6}]$:

$$Q \approx Q_o f(\alpha/\sqrt{6} - x_M/a_o) = kT \ln(\dot{\gamma}_o/\dot{\gamma}), \tag{4}$$

where Q_o, with dimension as energy, is a normalization constant and $\dot{\gamma}_o$ is another normalizing constant for the strain rate $\dot{\gamma}$. Combining Eqs. (2)–(4), we obtain the following expression for the critical strain to general defects:

$$\gamma = \frac{1}{A(T)}\left\{a_o\left[\frac{\alpha}{\sqrt{6}} - \beta(\dot{\gamma}, T)\right] \times \frac{1}{(\ln N)^{1/m}} - B(T)\right\}, \tag{5}$$

where

$$\beta(\dot{\gamma}, T) = f^{-1}((kT/Q_o) \times \ln(\dot{\gamma}_o/\dot{\gamma})) \tag{6}$$

is the inverse of the function f in Eq. (4) and is a constant at a given strain rate and temperature. f^{-1} is nondecreasing and so β increases with T and decreases with $\dot{\gamma}$.

In the MD conditions, the strain rate is very fast, so $\dot{\gamma} \rightarrow \dot{\gamma}_o$ and $\beta \rightarrow 0$. By setting $N = 31\,104$, which is the number of atoms used in the present MD supercell, $\beta = 0$, and A and B to the values given by the slopes and intercepts of the best straight lines in Fig. 2(b), the critical strain γ or simulation step at which defect generation occurs at a given T can be predicted from Eq. (5), with a suitable choice of α. It was found that by assuming $\alpha = 0.461$, Eq. (5) can predict very accurately the critical strains at which defect nucleation occurs in the simulations. The slight deviation of $\alpha = 0.461$ from the ideal value of 0.5 suggests that the barrier along the Shockley partial vector may not be symmetrical but has the hump occurring slightly earlier than the midpoint of the vector.

An interesting feature of the criterion in Eq. (5) is that the critical strain is predicted to be dependent on the volume of the material concerned through N, namely, if the material volume is increased, the critical strain should decrease, and vice versa. This, in fact, originates from statistics—in a larger collection of atoms, say, the chance of finding an atom exhibiting an extremely large relative displacement would be higher. Recently, Uchic *et al.* [2] studied the compressive stress-strain responses of $\langle 123 \rangle$-oriented Ni_3Al-Ta micropillars within the diameter range of 0.5 to 20 μm and aspect ratios from 2:1 to 4:1 and observed a marked increase in the yield point as the specimen size decreases. To see whether Eq. (5) can quantitatively describe their results, we calculate the sample sizes in the experiments by Uchic *et al.* according to $N = (\pi d^2/4) \times 3d \times (4/a_o^3)$, where d is the micropillar diameter, and an aspect ratio of 3:1 is assumed here which is the mean value used in the experiments by Uchic *et al.* Figure 3 shows the compressive yield strengths reported by Uchic *et al.,* plotted against the factor $(\ln N)^{-1/m}$, with m set to be 3.7. An apparent linear relationship is observed

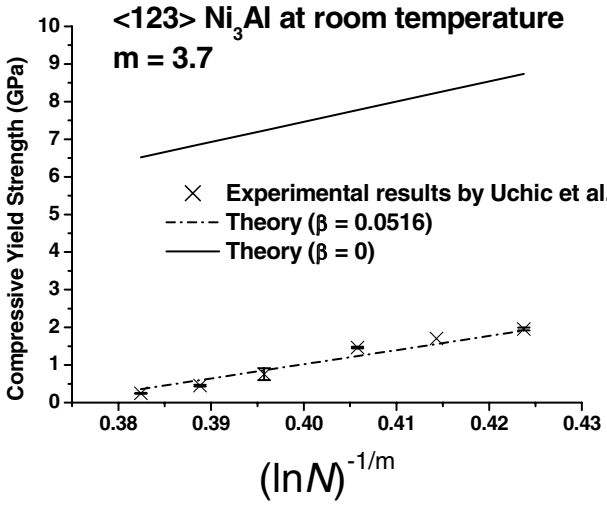

FIG. 3. Size dependence of compressive yield strength in Ni_3Al from the experiments by Uchic *et al.*

from the experimental data in Fig. 3, which qualitatively agrees with Eq. (5) if the shear strain is assumed to be proportional to the compressive yield strength. Indeed, before the onset of plasticity, the material behavior should be Hookean, and so the compressive yield strength should be $\sigma_c = MG\gamma$, where G is the shear modulus along the incipient slip system, M is a resolution factor connecting this slip system and the compression axis, and γ is that given by Eq. (5). For the $\langle 123 \rangle$ orientation used in the experiments by Uchic *et al.*, $M = 1.905$ if we assume a $\{111\}\langle 01\bar{1} \rangle$ slip system. Also, $G = 70.3$ GPa for the $\{111\}\langle 01\bar{1} \rangle$ slip system, calculated using the experimental elastic constants Voter and Chen used to fit their potentials [12]. The following parameters are also obtainable directly or indirectly from the MD simulations: $a_o = 0.3573$ nm, $\alpha = 0.461$, and $m = 3.7$, as discussed above, and $A = 0.174$ nm and $B = 0.0182$ nm as calculated from the slope and intercept of the best straight line in Fig. 2(b) at 300 K, the approximate temperature at which Uchic *et al.* performed their experiments. The only unknown parameter left in Eq. (5) is the strain-rate factor β. As shown in Fig. 3, excellent fit is obtained between the experimental values by Uchic *et al.* and Eq. (5) with a choice of $\beta = 0.0516$. Strain rate and the actual temperature are not reported in the paper by Uchic *et al.,* but, since the nanoindentation technique was used to compress the samples, the strain rate and temperature should not vary much in their work. Also, β in Eq. (6) depends more on the order of magnitude of $\dot{\gamma}$ rather than its actual value. Hence a constant β seems reasonable for the experimental results by Uchic *et al.*

Also shown in Fig. 3 is the prediction from Eq. (5) at extremely large strain rates corresponding to $\beta = 0$. Although similar size dependence also occurs, the σ_c values in this case are significantly higher than those measured in the experiments by Uchic *et al.* The predicted strengths at $\beta = 0$ are, in fact, the limiting strengths at ultrafast strain rates. Another obvious limit of Eq. (5) is that when the specimen size keeps decreasing, the predicted strength would approach the ideal strength, of the order of $G/10$. At this point, direct rupture of atomic bonds might take over defect nucleation. For bulk sized specimens, Eq. (5) would also not be applicable since the chance of existence of initial crystal defects would no longer be negligible and hence incipient plasticity would occur via heterogeneous nucleation.

To conclude, the results here suggest that dislocation generation occurs in a micron-sized material volume by having one individual atom achieving a critical relative displacement with respect to its neighbors through the combined effects of thermal agitation and a large applied strain.

This research was supported by a research grant (No. HKU 7201/03E) from the Research Grants Council, Hong Kong Special Administrative Region of People's Republic of China.

[1] N. A. Fleck, G. M. Muller, M. F. Ashby, and J. W. Hutchison, Acta Metall. Mater. **42**, 475 (1994).
[2] M. D. Uchic, D. M. Dimiduk, J. N. Florando, and W. D. Nix, Science **305**, 986 (2004).
[3] See, for example, R. E. Smallman and R. J. Bishop, *Metals and Materials—Science, Processes, Applications* (Butterworth-Heinemann, Oxford, 1995), p. 223.
[4] W. W. Gerberich, S. K. Venkataraman, H. Huang, S. E. Harvey, and D. L. Kohlstedt, Acta Metall. Mater. **43**, 1569 (1995).
[5] C. A. Schuh and A. C. Lund, J. Mater. Res. **19**, 2152 (2004).
[6] P. C. Wo, L. Zuo, and A. H. W. Ngan, J. Mater. Res. (to be published).
[7] Y. L. Chiu and A. H. W. Ngan, Acta Mater. **50**, 1599 (2002).
[8] G. Feng, Master's thesis, University of Hong Kong, 2001.
[9] Wo *et al.* [6] found that the statistical distribution of the waiting times for yielding to occur in this situation did not obey predictions from a homogeneous nucleation theory but exhibited characteristics of an accumulative damage model.
[10] J. Li, K. J. Van Vliet, T. Zhu, S. Yip, and S. Suresh, Nature (London) **418**, 307 (2002).
[11] J. Li, T. Zhu, S. Yip, K. J. Van Vliet, and S. Suresh, Mater. Sci. Eng. A **365**, 25 (2004).
[12] A. F. Voter and S. P. Chen, in *Characterization of Defects in Materials*, edited by R. W. Siegel, J. R. Weertman, and R. Sinclair, MRS Symposia Proceedings No. 82 (Materials Research Society, Pittsburgh, PA, 1987), p. 175.
[13] L. V. Woodcock, Chem. Phys. Lett. **10**, 257 (1970).
[14] M. F. Horstemeyer, M. I. Baskes, and S. T. Plimpton, Acta Mater. **49**, 4363 (2001).
[15] M. P. Allen and D. J. Tildesley, *Computer Simulation of Liquids* (Clarendon Press, Oxford, 1987), p. 60.
[16] A. H. W. Ngan, M. Wen, and C. H. Woo, Comput. Mater. Sci. **29**, 259 (2004).